

Wide Area Deposition of Transparent Flexible Nanocomposites

T. Druffel

Optical Dynamics Nanotechnology, 1950 Production Ct., Louisville, KY 40299, USA
tdruffel@opticaldynamics.com

ABSTRACT

Inorganic-organic nanocomposites offer a multitude of options to engineer abrasion resistance, improve UV weathering, enhance thermal conductivity, and control refractive index. Enhancements of this kind are typically only achieved if the nanoparticles are randomly dispersed as discrete entities within the polymer matrix. This constraint requires tight control of nanoparticle synthesis and chemical modification of the nanoparticle surface for appropriate polymerization within the matrix. Metal oxide nanocomposite coatings are distinguished by their high visible transparency and preservation of polymer flexibility. In this paper we discuss the deposition of nanocomposite coatings using techniques that are suitable for large and small areas. We also explore specific material properties and the behavior of these coatings under large strains.

Keywords: Nanocomposite, Thin Film, Flexible, Deposition

1 INTRODUCTION

Nanocomposites with various refractive indices and mechanical properties are produced by using different monodisperse inorganic nanoparticles in an optimized polymer matrix. A self-assembled polymer nanocomposite coating composed of metal oxide nanoparticles and a UV-cured acrylate has been developed for flexible applications requiring high visible transparency. This commercial coating includes the hardware, process and chemistry to provide a broadband anti-reflective filter spanning the visible wavelengths for independent opticians and to date there are nearly 100,000 people wearing these nanocomposite coatings in the United States and Worldwide [1]. The strain domains of these films are very similar to those of the polymer substrate and as such do not exhibit the crazing or cracking often associated with films applied through vapor deposition [2]. These coatings perform well on flexible substrates as shown in Figure 1, and phenomenal flexibility has also been demonstrated on 38-layer films on a urethane substrate strained in excess of 25% without film failure. The refractive index of the coatings can be manipulated by changing the packing density of the nanoparticles, and tight control of the particle diameters results in highly transparent films.

A recent review of thin films in solar energy discussed several applications of transparent conductors [3] that could be fulfilled with nanocomposites. Photovoltaic devices

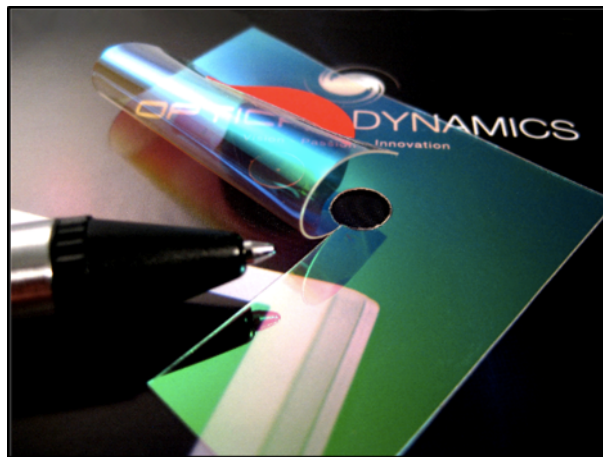


Figure 1. Multilayer film on flexible substrate

utilizing nanoparticles have been demonstrated, and devices using metal and metal oxide nanoparticles in which electromagnetic radiation is transmitted, reflected, concentrated or absorbed can replace more expensive physical vapor deposited (PVD) materials. To move the nanocomposite technology towards sustainable and renewable requires that the films be produced across wide areas. Roll-to-roll techniques are aptly suited for deposition of nanocomposite thin films over wide area substrates. These flexible systems and deposition techniques open applications of sustainable and renewable solar applications on three dimensional surfaces.

We will discuss the chemistry, process and equipment needed to move the evaporative spin coating of nanocomposites to cover wide areas. The deposition represents a significant reduction in costs and offers a versatile process to cover a number of film depositions. The process is capable of depositing highly transparent films of distinct refractive index as shown in figure 2 which is a feasibility of the concept by depositing a nanocomposite with approximately a 45 percent nanoparticles by spray coating. The thickness of the film was measured to be several microns thick and the refractive index of the coating was determined to be approximately 1.75. The coating has been scraped from each end of the slide, and it is evident from the reflectance of the light that the center section has a higher refractive index. This demonstration shows that transparent nanocomposites can be deposited utilizing printing technique without agglomeration of the particles even at high packing densities.



Figure 2: Demonstration of a nanocomposite coating deposited using a micro fluid dispensing valve.

2 BACKGROUND

The primary optical property of a material is its refractive index. This simple ratio is used to explain the propagation of electromagnetic waves through materials and at interfaces. The design and production of optical filters is mainly accomplished through the combination of thin films with unique refractive indices. These are typically dielectric and metal films that are almost exclusively deposited using vacuum deposition. Although these materials have been studied extensively, they have significant disadvantages related to the processing steps and limited mechanical flexibility. The nanocomposites composed of inorganic nanoparticles embedded in an organic polymer matrix directly address these issues. The challenges for nanocomposites are to alter the optical properties of a material without affecting the visible transparency of the final article. The need and methods to build nanocomposites of randomly dispersed nanoparticles for high visible transparency is discussed. The need for discrete dispersions of nanoparticles in the polymer matrix will be discussed along with methods to maintain the separation between the nanoparticles.

2.1 Nanocomposites

Nanocomposites composed of inorganic nanoparticles in a polymer matrix offer a unique platform to engineers, in such that the optical and mechanical properties of the composites can be changed. Nanocomposites with various refractive indices and mechanical properties are produced using different monodisperse inorganic nanoparticles in an optimized polymer matrix [4]. The strain domains of these films are very similar to those of the polymer substrate and as such do not exhibit the crazing or cracking often associated with films applied through vapor deposition. There is no need to use high heats to establish the coating, thus processing on plastics is straightforward. Inorganic-

organic nanocomposites can be assembled from three distinct components: crystalline nanoparticles, polymers and organometallics as shown in the Venn diagram (see Figure 3). The organometallics are the precursor chemistries for the sol-gel process and can be used solely to produce thin film filters. Starting with crystalline nanoparticles to produce an inorganic-organic nanocomposite can be done by simply incorporating a colloidal dispersion of nanoparticles into a monomer and curing. The limitation to this method is that the nanoparticles do not actively participate in the curing, and so a homogeneous material is not formed. Yu et. al. produced thin films on the order of several microns using a colloidal silica and acrylic monomer cured in the presence of heat [5]. Others have developed nanoparticle based layers into an antireflective coating by spin coating and layer by layer deposition [6,7].

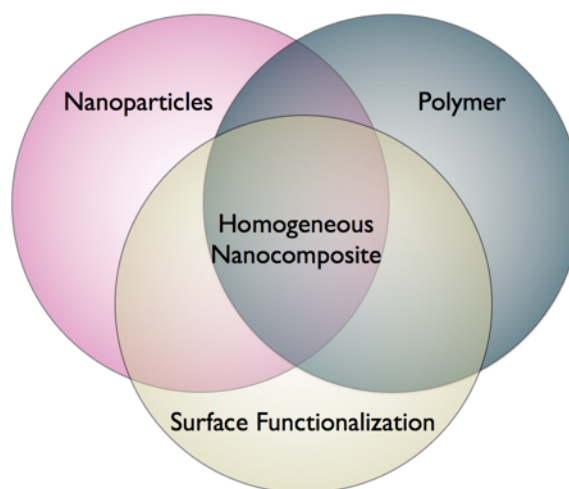


Figure 3: Venn Diagram of an inorganic-organic nanocomposite.

Steric stabilization of the nanoparticles through surfactants or polymer surfaces reduces the surface energy of the nanoparticles and can result in inferior coatings. By functionalizing the crystalline nanoparticles with a polymerizable group, chemical bonds between the nanoparticles and the polymer matrix are formed. This creates a route to produce a homogeneous dispersion of nanoparticles in a polymer matrix which is the key to producing nanocomposites that have high visible transparency while maintaining the elastic properties of the polymer.

2.2 Engineered Properties

The optical and mechanical properties of a nanocomposite are engineered by varying the volume concentration of nanoparticles in the matrix. Using spin coating techniques these properties can be engineered from the base polymer up to 65 volume percent, nearly the

theoretical close packing of spheres. The spin coating method is a well understood deposition technique that produces reproducible uniform films that are spread across a substrate with considerable shear forces. When the optical diameter of the nanoparticles becomes to large, optical scattering results as the light waves are reflected from the boundary of the inorganic and organic phases.

The refractive index of a nanocomposite that is a homogeneous mixture of an inorganic metal oxide nanoparticle and an organic polymer can be modeled as a mixture of the two. The refractive index of a material is related to the square root of the permittivity and the permittivity of a composite material is equivalent to the average of the components. Thus the refractive index of a composite material is related as:

$$n^2 = \sum_i n_i^2 v_i \quad (1)$$

Where n_i and v_i are the refractive index and volume fractions of the components [8]. Although there are numerous relations modeling the mixture of two discrete materials the following is sufficient for most modeling purposes. So by knowing the refractive index of the two materials modeling software can be used to determine the refractive index of a thin film nanocomposite.

The inorganic nanoparticles have a non-uniform refractive index across the visible spectrum, whereas the organic polymer is near constant across the spectrum. Nanocomposite films approximately 500 nm thick with refractive indices between 1.5 and 1.75 measured at 480 nm were made using ZnO nanoparticles a 5 to 50% loading of nanoparticles and a UV curable monomer as shown in figure 4. The films used ZnO dispersed in TMPTA at varying volume loadings and spun coated onto a quartz substrate using the Optical Dynamics spin coater. The source of the ZnO is a nanoparticle dispersion in methyl ethyl ketone (MEK) by Umicore (Zano MEK 067) which is reported to have 30 nm ZnO nanoparticles dispersed at 45 weight percent. The dispersion uses a surfactant to maintain the nanoparticle separation. The refractive index was determined by measuring the reflectance spectrum using a contact spectrophotometer F20 by Filmetrics and measuring the thickness and roughness using a contact profilometer XP-1 by Ambios corporation. This data was then used to determine the refractive index using a Cauchy model. It should be noted that the refractive index of the fully loaded ZnO film has been determined to be approximately 1.75, which is slightly lower than the expected 1.82. This is most likely due to the added surfactant reducing the effective refractive index of the ZnO nanoparticles. A similar study of TiO₂ nanocomposite films was undertaken and resulted in a maximum refractive index of 1.88 at a volume packing of 65 volume percent. These films were used to produce thin film reflective filters with up to 38 layers and strained up to 25 percent [9].

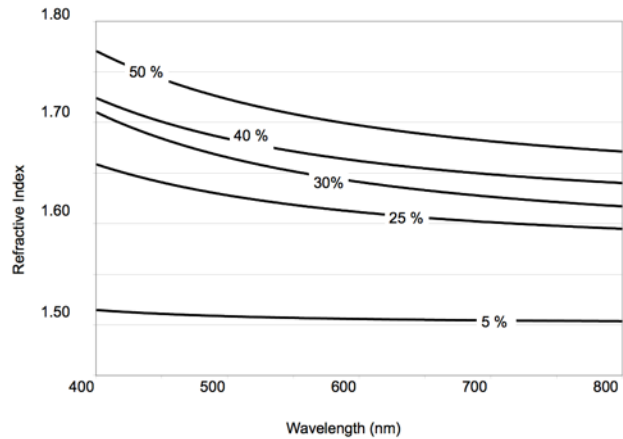


Figure 4: Refractive index dispersion of nanocomposites featuring varying volume fractions of ZnO dispersed in a UV cured polyurethane acrylate.

Another use of nanocomposite films would be as absorptive filters that maintain a high visible transparency. Examples of these would be eye protection from harmful ultra violet and infra red wave-lengths. Metal oxides also have high absorption in the UV region, this coupled with the low absorption in the visible region makes these ideal for optical applications requiring UV blocking. It is well known that titanium dioxide and ZnO have very high absorption in the ultra- violet region. The optical and UV response of 500 nm thick ZnO films of varying volume ratios of ZnO nanoparticles was measured using a UV-Vis spectrophotometer 8453 by Hewlett Packard. As anticipated the ZnO dispersions had a solid edge at about 380 nm which is in line with what is expected of the UV absorbance of ZnO. The UV absorbance ($\lambda = 340$ nm) of the ZnO was linear with the volume fraction of ZnO in the films.

A similar study of the impact of volumetric loading of nanoparticles on the modulus of a thin film resulted in a maximum modulus of near 60 percent loading [10]. In this study silica nanoparticles were dispersed at volumes ranging from 30 to 75 percent by volume and the modulus was measured using nanoindentation.

3 DEPOSITION

All of the films discussed above were spin coated onto 80 mm substrates using a piece of equipment that was specifically designed to deposit thin film nanocomposites. The coater moves up to four separate 80 mm diameter substrates through three process steps: cleaning, coating, and curing. All of the coating parameters (spin speed, air flow, temperature, and sweep) are computer controlled, with the solvent being removed from the coating chamber using a fan. After the coating is applied, the films are cured using a pulsed xenon strobe lamp. All of these parameters must be considered when designing large area deposition.

Spin coating is not an ideal candidate for large area substrates, and thus the engineer is faced with depositing

high volume density films without a simply applied force to overcome the thermodynamic surface forces of the nanoparticles. The stabilization techniques used to keep the nanoparticles dispersed in a solvent may not translate into a discrete dispersion in the nanocomposite. Ideally, the functionalization would reduce the surface energy of the nanoparticles to be equivalent to the monomers creating a bulk nanocomposite monomer.

The deposition of thin films using dip coating would be an ideal application of these nanocomposites for large area substrates. A simple set-up was built to pull a glass slide out of a nanoparticle dispersion at speeds between 1 and 25 mm/s. The nanocomposite dispersion was a Cerium dioxide, which is available as a colloidal suspension from Sigma-Aldrich (Product No 289744) and a Trimethylolpropane Triacrylate. The ceria dispersion was functionalized such that acrylate groups surrounded the nanoparticles. The total volume of the nanoparticles was 40 percent. The thickness of the coating was determined to be 270 nm, with a refractive index of 1.8 measured at 480 nm. The composition was then diluted to produce a film that would be on the order of a quarter wavelength (approximately 70 nm) shown in figure 5b. This was then alternately dipped between a high (CeO₂) and low (SiO₂) nanocomposite to build a nine layer reflective coating (figure 5a).

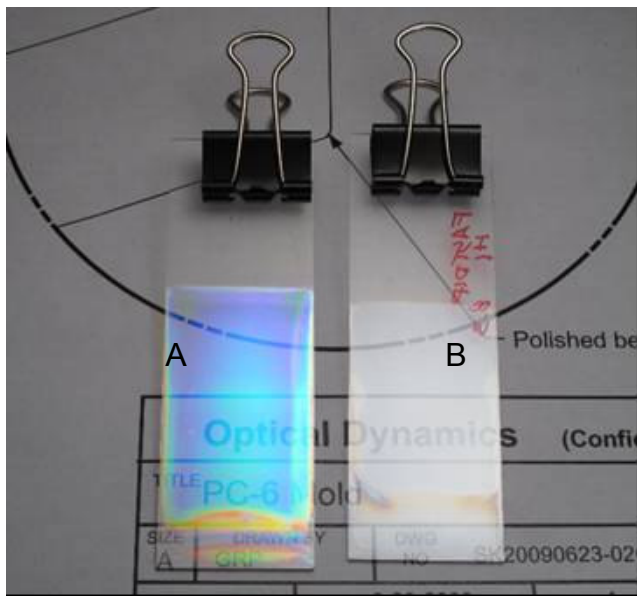


Figure 5: Dipped coated thin films of CeO₂ (right b) and CeO₂ and SiO₂ (left a).

Roll-to-roll methods such as Gravure, knife blade and spray to deposit these coatings on flexible substrates has also been employed. These methods as well as the dip coating method mentioned earlier do not use high shear forces to aid in the homogenous dispersion of the thin films, and so the surface functionalization is important. A demonstration of a roll-to-roll mirror is shown in figure 6.

The color variations across the mirror are due to PET substrate not being flat.

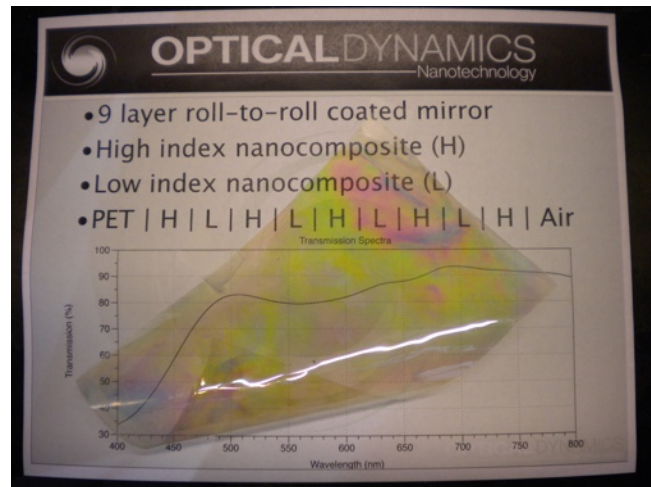


Figure 6: Nanocomposite thin film mirror deposited onto a flexible PET substrate

4 CONCLUSION

The results show that metal oxide nanoparticles can be used to engineer important material properties of thin films. These films can be deposited onto very flexible substrates using methods that are very amenable to in-line wide area deposition. Furthermore, the deposition techniques are carried out at very near atmospheric conditions.

REFERENCES

- [1] Druffel, T., et al., **2006**, United States Patent Application No. 20060065989
- [2] Druffel, T., Geng, K., Grulke, E., **2006** *Nanotechnology*, 17(14): p. 3584.
- [3] Granqvist, C.G., **2007**, *Solar Energy Materials and Solar Cells*, 91: p. 1529
- [4] Krogman, K., Druffel, T., Sunkara, M., **2005**, *Nanotechnology*, 16, S338
- [5] Yu, Y.-Y., Chen, W.-C., **2003**, *Materials Chemistry and Physics*, 82, p. 388
- [6] Gemici, Z., Shimmer, H., Cohen, R. E., Rubner, M. F., **2008**, *Langmuir*, 24 (5), p. 2168
- [7] Lee, D., Rubner, M. F., Cohen, R. E., **2006**, *Nano Letters*, 6 (10) p. 2305
- [8] Yamasaki, T., Tsetse, T., 1998, *Applied Physics Letters*, 72, p. 1957
- [9] Druffel, T., Lattis, M., Spencer, M., Buazza, O., **2010**, *Nanotechnology*, 21 in press
- [10] Druffel, T., Mandzy, M., Sunkara, M., Grulke, E., 2008, *Small*, 4 (4) p. 459